

Role of Cation Size in the Energy of Electron Transfer to 1:1 Polyoxometalate Ion Pairs $\{(M^+)(X^{n+}VW_{11}O_{40})\}^{(8-n)-}$ ($M = Li, Na, K$)

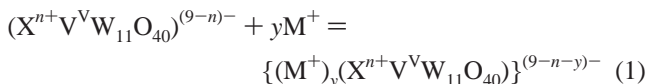
Vladimir A. Grigoriev, Craig L. Hill,* and Ira A. Weinstock*†

Department of Chemistry, Emory University
Atlanta, Georgia 30322

Received November 1, 1999

The use of soluble salts of polyoxometalates (d^0 -early-transition metal oxygen-anion clusters or POMs) as selective oxidation or electron-transfer catalysts, as probes in physical-organic and biological chemistry, and in the study of electron- and energy-transfer phenomena constitutes a substantial and rapidly growing literature.¹ While rarely addressed,² however, POM solutions contain equilibrium distributions of free anions and ion-paired structures of variable stoichiometry. Thus, although studies of crystalline POM salts used in heterogeneous catalysis clearly indicate that cation–anion interactions dramatically alter POM properties in these static ideal cases,³ the influence of ion pairing on POM reactions in solution is often ignored. Even in reports that document the influence (typically on reaction rates) of added cations, the relationship between observed effects and the properties of specific solution-POM structures is left to conjecture.⁴ Partly to blame is the difficulty encountered in determining the extent and stoichiometry of ion-pair formation, a necessary prerequisite for assigning physical properties to specific solution-POM structures.⁵

We herein report that by carefully controlling POM size, structure and charge, solvent, temperature, buffer and electrolyte composition, and concentration, we have prepared a series of nine 1:1 association complexes between alkali-metal cations (Li^+ , Na^+ , and K^+) and three representative vanadium(V)-substituted α -Keggin heteropolytungstates, α -($X^{n+}VW_{11}O_{40}$)⁽⁹⁻ⁿ⁾⁻ ($X = P(V), Si(IV),$ and $Al(III)$) (eq 1; $y = 1$). As a result of these efforts,



formal $1e^-$ -reduction potentials, a key thermodynamic property associated with rates of electron and energy transfer, are for the first time assigned to specific 1:1 ion pairs. Reduction potentials of the solvated ion pairs increase in the order $E^{\circ}_{LiPOM} < E^{\circ}_{NaPOM} < E^{\circ}_{KPOM}$. At the same time, the effective hydrodynamic radii, r , of the association complexes decrease in the order $r_{LiPOM} >$

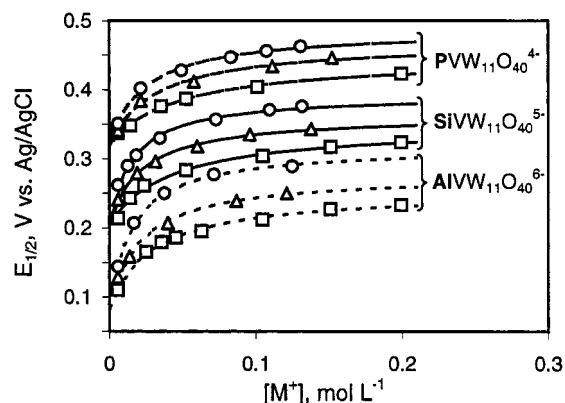


Figure 1. Plot of $E_{1/2}$ vs $[M^+]$: $M^+ = Li^+$ (\square), Na^+ (Δ), and K^+ (\circ); $[M^+]$ = total cation concentration from MCl, POM counteranions, and buffer.

$r_{NaPOM} > r_{KPOM}$, a result that establishes a correlation between increasing electron affinity and the formation of smaller (more intimate) ion pairs.

As the equilibrium in eq 1 is shifted to the right by addition of M^+ , the reduction potential, E , of the solution moves to more positive values. For $y = 1$, the increase in E is described by a rectangular hyperbolic function⁶ (eq 2; derived by linear combination of molar Gibbs free energy terms and $\Delta G = -nFE$). In eq

$$E = (E_{POM} + E_{MPOM}K_{MPOM}[M^+]) / (1 + K_{MPOM}[M^+]) \quad (2)$$

2, E_{POM} is the formal $1e^-$ -reduction potential of the unpaired anion (i.e., the $(X^{n+}VW_{11}O_{40})^{(9-n)-} / (X^{n+}VW_{11}O_{40})^{(10-n)-}$ couple), E_{MPOM} is the analogous reduction potential of the 1:1 ion pair, $K_{MPOM} = \{[(M^+)(X^{n+}VW_{11}O_{40})]^{(8-n)-} / [M^+][(X^{n+}VW_{11}O_{40})^{(9-n)-}]\}$, and $[M^+]$ is the equilibrium concentration of the alkali-metal cation. Pure samples of the nine POM salts studied, α - $M^{(9-n)-}$ ($X^{n+}VW_{11}O_{40}$) ($X = P(V), Si(IV),$ and $Al(III)$; $M^+ = Li^+, Na^+,$ and K^+), were prepared.⁷ Solutions of each of the nine salts (1.0 mM) in minimally (1.0 mM) acetate-buffered 2:3 v/v (3.54:1.00 molar ratio) H_2O :*tert*-butyl alcohol solutions (the water components were first adjusted to pH 4.76 using HOAc and MOAc, $M^+ = Li^+, Na^+,$ or K^+) were heated to 60 °C under argon. Cyclic voltammograms (Figure 1; 55 measurements in all) were obtained as alkali-metal concentrations were gradually increased by additions of LiCl, NaCl, or KCl.⁸ The data in Figure 1 were fit to eq 2 (fitted curves) by nonlinear regression⁹ using the Solver program in Microsoft Excel. Agreement between experimental data and eq 2 over statistically meaningful $[M^+]$ values¹⁰ is the first line of evidence in support of the stoichiometry shown in eq 1. Second, as $[M^+]$ values decrease, the nine curves in Figure 1 converge to three E_{POM} values, the reduction potentials of the three unpaired anions ($X = P, Si,$ and Al) on the left side of eq 1.

(6) Connors, K. A. *Binding Constants: The Measurement of Molecular Complex Stability*; John Wiley & Sons: New York, 1987; pp 59–69 and Appendix A, pp 373–384.

(7) K^+ salts: (a) Domaille, P. J. *J. Am. Chem. Soc.* **1984**, *106*, 7677–7687. $K_3P^{IV}W_{11}O_{40}$ and $K_6Si^{IV}W_{11}O_{40}$ were oxidized with Br_2 in water to $K_4P^{V}W_{11}O_{40}$ and $K_5Si^{V}W_{11}O_{40}$. (b) Weinstock, I. A.; Cowan, J. J.; Barbuzzi, E. M. G.; Zeng, H.; Hill, C. L. *J. Am. Chem. Soc.* **1999**, *121*, 4608–4617. Li^+ and Na^+ salts were obtained by ion-exchange chromatography (Li^+ or Na^+ forms of Amberlite IR-120 (plus) ion-exchange resin).

(8) A BAS CV-50W was used with glassy-carbon (working), Pt (auxiliary), and Ag/AgCl (3 M NaCl) (reference) electrodes; formal reduction potentials, $E_{1/2} = (E_{cathodic} + E_{anodic})/2$, are reported vs Ag/AgCl. Nearly electrochemically reversible behavior observed in the “plateau” regions in Figure 1 (ΔE values near theoretical of 66 mV at 60 °C; 100 mV/s sweep rate) provides precise E_{MPOM} values (from eq 2) despite uncertainties in E_{POM} at low $[MCl]$ (ΔE values of 133 ($X = P, Si$) to 220 mV ($X = Al$)).

(9) $[M^+]$ values shown in Figure 1 and used to fit the data to eq 2 are the sum of $[M^+]$ from initially added MCl, POM counteranions, and buffer.

† Visiting scientist at Emory University (1996–2000). Permanent address: U.S. Forest Service, Forest Products Laboratory, Madison, WI 53705.

(1) (a) Pope, M. T.; Müller, A. *Angew. Chem., Int. Ed. Engl.* **1991**, *30*, 34–48. (b) Pope, M. T.; Müller, A. *Polyoxometalates: From Platonic Solids to Anti-Retroviral Activity*; Kluwer Academic Publishers: Dordrecht, 1994. (c) Hill, C. L.; Prosser-McCartha, C. M. *Coord. Chem. Rev.* **1995**, *143*, 407–455. (d) Okuhara, T.; Mizuno, N.; Misono, M. *Adv. Catal.* **1996**, *41*, 113–252. (e) Hill, C. L., Ed. Special thematic issue on polyoxometalates. *Chem. Rev.* **1998**, *98*, 1–389. (f) Neumann, R. *Prog. Inorg. Chem.* **1998**, *47*, 317–370.

(2) Kirby, J. F.; Baker, L. C. W. *Inorg. Chem.* **1998**, *37*, 5537–5543. (3) (a) Prosser-McCartha, C. M.; Kadkhodayan, M.; Williamson, M. M.; Bouchard, D. A.; Hill, C. L. *J. Chem. Soc., Chem. Commun.* **1986**, 1747–1748. (b) Williamson, M. M.; Bouchard, D. A.; Hill, C. L. *Inorg. Chem.* **1987**, *26*, 1436–1441. (c) Hill, C. L.; Bouchard, D. A.; Kadkhodayan, M.; Williamson, M. M.; Schmidt, J. A.; Hilinski, E. F. *J. Am. Chem. Soc.* **1988**, *110*, 5471–5479. See also: (d) Inumaru, K.; Ito, T.; Misono, M. *Microporous Mesoporous Mater.* **1998**, *21*, 629–635. (e) Ouahab, L. *Coord. Chem. Rev.* **1998**, *180*, 1501–1531. (f) Coronado, E.; Gómez-García, C. J. *Chem. Rev.* **1998**, *98*, 273–296.

(4) Weinstock, I. A. *Chem. Rev.* **1998**, *98*, 113–170.

(5) (a) Ebersson, L. *J. Am. Chem. Soc.* **1983**, *105*, 3192–3199. (b) Hiskia, A.; Papaconstantinou, E. *Inorg. Chem.* **1992**, *31*, 163–167. (c) Toth, J. E.; Anson, F. C. *J. Electroanal. Chem.* **1988**, *256*, 361–370.

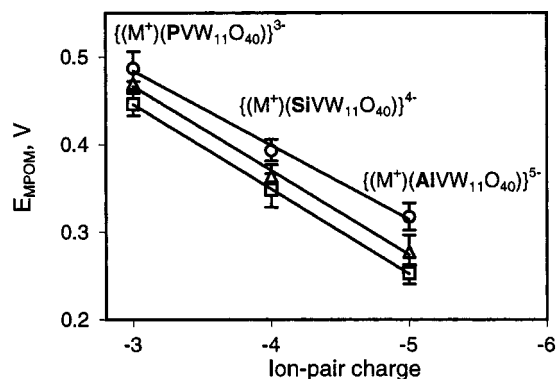


Figure 2. Plot of E_{MPOM} vs ion-pair charge; $M^+ = Li^+$ (\square), Na^+ (Δ), and K^+ (\circ).

The third line of evidence is obtained by recourse to Pope's observation¹¹ that reduction potentials of isostructural Keggin anions in solution decrease linearly with whole-number increments in anion charge. Similarly, the reduction potentials of identically charged ion pairs $\alpha\text{-}\{(M^+)(X^{n+}VW_{11}O_{40})\}^{(8-n)-}$, i.e., $M^+ = Li^+$, Na^+ , or K^+ , should decrease linearly with overall complex-anion charge in the order $\{(M^+)(PVW_{11}O_{40})\}^{3-} > \{(M^+)(SiVW_{11}O_{40})\}^{4-} > \{(M^+)(AlVW_{11}O_{40})\}^{5-}$. E_{MPOM} values associated with the nine curves in Figure 1 (fit to eq 2) are plotted as a function of overall anion charge in Figure 2.¹² The linear decrease in reduction potential as the heteroatom, X, is varied from P(V) (upper left) to Al(III) (lower right) directly establishes the stoichiometry in eq 1 and confirms the applicability of eq 2. As a result, we can now compare the reduction potentials, E_{MPOM} , of the nine unique 1:1 ion pairs: For each heteroatom, X, in $\{(M^+)(X^{n+}VW_{11}O_{40})\}^{(8-n)-}$, reduction potentials increase with counteranion size in the order $M^+ = Li^+ < Na^+ < K^+$.

As reduction potentials increase, the solvated ion pairs themselves decrease in size in the order $M^+ = Li^+ > Na^+ > K^+$. Relative sizes (molecular volumes) were approximated as effective hydrodynamic radii using the Stokes–Einstein equation, $D = kT/6\pi\eta r$, where D is the diffusion coefficient of a sphere of radius r in a solvent of viscosity η .¹³ Diffusion coefficients, D , were determined using single-potential-step chronoamperometry (CA).¹⁴

(10) An acceptable test of the 1:1 stoichiometry in eq 1 requires measurement of the binding isotherm ($E_{1/2}$ values in the present case) and agreement with the rectangular hyperbolic function (eq 2) from 20 to 80% of complete saturation: (a) Deranleau, D. A. *J. Am. Chem. Soc.* **1969**, *91*, 4044. (b) Deranleau, D. A. *J. Am. Chem. Soc.* **1969**, *91*, 4050.

(11) (a) Pope, M. T.; Varga, J.; Gideon, M. *Inorg. Chem.* **1966**, *5*, 1249–1254. (b) Altenau, J.; Pope, M. T.; Prados, R. A.; So, H. *Inorg. Chem.* **1975**, *14*, 417–421.

(12) The confidence intervals plotted in Figure 2 (ca. 95%) were taken from 2-dimensional sum-of-squares contours defined by variation in K_{MPOM} and E_{MPOM} (method of analysis of variance: Box, G. E. P.; Hunter, W. G.; Hunter, J. S. *Statistics for Experimenters*; Wiley: New York, 1978; p 469).

(13) The hydrodynamic radii of Keggin anions determined from diffusion coefficients by use of the Stokes–Einstein equation are the same as those obtained by velocity ultracentrifugation and from viscosity and density data: (a) Baker, M. C.; Lyons, P. A.; Singer, S. J. *J. Am. Chem. Soc.* **1955**, *77*, 2011–2012. (b) Kurucsev, T.; Sargeson, A. M.; West, B. O. *J. Phys. Chem.* **1957**, *61*, 1567–1569. Application of Stokes–Einstein to nonspherical (but similarly shaped) ions provides an internally consistent means of interpreting hydrodynamic data (diffusion coefficient, D , values: (c) Edward, J. T. *J. Chem. Educ.* **1970**, *47*, 261–270) and for visualizing the relative molar volumes associated with specific D values.

(14) Starting with 1.0 mM solutions of $(X^{n+}VW_{11}O_{40})^{(9-n)-}$ (Li^+ , Na^+ , and K^+ salts) in pure water (25 °C) and in H_2O :*tert*-butyl alcohol (60 °C), quantities of LiCl (137 mM, X = P; 202 mM, X = Si), NaCl (110 mM, X = P, Si) and KCl (90 mM, X = P; 85 mM, X = Si) associated with 93% 1:1 ion-pair formation in H_2O :*tert*-butyl alcohol were added (i.e., 93% saturation based on eqs 1 and 2, see Figure 1). Due to solubility limits, 90% saturation (160 mM LiCl, 121 mM NaCl, and 92 mM KCl) was used for $\{(M^+)(AlVW_{11}O_{40})\}^{5-}$. Diffusion coefficients were determined from the plateau values of $it^{1/2}$ vs t plots (from $i = nFAD^{1/2}C^*/\pi^{1/2}t^{1/2}$, the Cottrell equation), with $C^* = [(X^{n+}VW_{11}O_{40})^{(9-n)-}]_{total}$; the area, A, of the horizontal electrode was determined using $[K_4(Fe(CN)_6)]_{aq}$ in 2.0 M KCl (Adams, R. N. *Electrochemistry at Solid Electrodes*; Marcel Dekker: New York, 1969; pp 213–219).

Table 1. Diffusion Coefficients, Effective Hydrodynamic (Stokes–Einstein) Radii, and Reduction Potentials of

$\{(M^+)(X^{n+}VW_{11}O_{40})\}^{(8-n)-}$ (X = P(V), Si(IV), Al(III)); $M^+ = Li^+$, Na^+ , K^+) Ion Pairs^a

ion pair					
X	M	$10^2\eta$, P	10^6D , cm ² /s	r_{eff} , Å	E_{MPOM} , mV ^b
P	Li	1.41 ± 0.01	2.38 ± 0.05	7.2 ± 0.2	446 ± 14
	Na	1.41 ± 0.01	2.46 ± 0.07	6.9 ± 0.3	470 ± 13
	K	1.39 ± 0.01	2.78 ± 0.11	6.2 ± 0.3	487 ± 17
Si	Li	1.40 ± 0.01	2.08 ± 0.10	8.3 ± 0.4	348 ± 19
	Na	1.34 ± 0.01	2.33 ± 0.05	7.7 ± 0.2	364 ± 13
	K	1.37 ± 0.01	2.56 ± 0.09	6.8 ± 0.3	393 ± 13
Al	Li	1.43 ± 0.01	1.64 ± 0.05	10.3 ± 0.4	252 ± 11
	Na	1.39 ± 0.01	1.74 ± 0.05	9.8 ± 0.3	277 ± 18
	K	1.39 ± 0.01	1.79 ± 0.05 ^c	9.6 ± 0.3 ^c	317 ± 16

^a H_2O :*tert*-butyl alcohol (2:3 v/v) at 60 °C. ^b Ag/AgCl (3 M NaCl) reference electrode. ^c Due to adsorption on the electrode surface, the actual D value may be larger (and r_{eff} value smaller) than that listed.

In pure water, diffusion coefficients of the three Keggin anions (MCl concentrations corresponding to the plateau regions in Figure 1; nine aqueous solutions) are the same for added LiCl, NaCl, or KCl and give Stokes–Einstein radii (5.7 ± 0.3 , 5.6 ± 0.2 , and 5.9 ± 0.2 Å for X = P(V), Si(IV), and Al(III)) of unpaired anions (cf. 5.6 Å for $(PW_{12}O_{40})^{3-}$ and $(SiW_{12}O_{40})^{4-}$).^{11a} However, upon induction of 1:1 ion-pair formation by use of 2:3 v/v H_2O :*tert*-butyl alcohol at 60 °C, diffusion coefficients and effective Stokes–Einstein radii now vary with the nature of M^+ (Table 1). For each heteroatom, X, diffusion coefficients of the $\{(M^+)(X^{n+}VW_{11}O_{40})\}^{(8-n)-}$ ion pairs increase with alkali-metal cation size in the order $M^+ = Li^+ < Na^+ < K^+$, while effective radii ($D \propto 1/r$) decrease accordingly. Although the effective crystallographic (Shannon and Prewitt) radii of hexacoordinate Li^+ , Na^+ , and K^+ ions increase respectively from 0.90 to 1.16 to 1.52 Å,¹⁵ the solvated radii of these ions decrease with charge density, e/r , in the same order.¹⁶ Thus, the effective sizes of the solvated cations in the 1:1 ion pairs (and hence, cation–anion distances) decrease as the “naked” alkali-metal cation radii become larger:¹⁷ solvated Li^+ forms the largest ion pairs and solvated K^+ the smallest (most intimate) association complexes. These data provide a structural basis for the greater electron-transfer⁴ (substrate oxidation) rates¹⁸ associated with larger alkali-metal cations. The larger and less extensively solvated alkali-metal cations form smaller (more intimate) association complexes that possess larger electron affinities.

Acknowledgment. We thank Dr. Carl J. Houtman for nonlinear regression error-analysis software and the DOE (DE-FC36-95GO10090 to I.A.W. and C.L.H.) and the NSF (CHE-9412465 to C.L.H.) for support. JA993862C

(15) Shannon, R. S.; Prewitt, C. T. *Acta Crystallogr.* **1969**, *B25*, 925–946.

(16) For example, the approximate hydrated radii of Li^+ , Na^+ , and K^+ in water decrease from 3.40 to 2.76 to 2.32 Å as the approximate waters of hydration decrease from 25.3 to 16.6 to 10.5: (a) Stern, K. H.; Amis, E. S. *Chem. Rev.* **1959**, *59*, 1–64. (b) Cotton, F. A.; Wilkinson, G. *Advanced Inorganic Chemistry*, 4th ed.; Wiley: New York, 1980; p 255.

(17) (a) Metelski, P. D.; Swaddle, T. W. *Inorg. Chem.* **1999**, *38*, 301–307. See also Baker's interpretation of ³¹P NMR spectral data reported in ref 2. Increases in size from X = P(V) to Al(III) are consistent with pronounced increases in hydrodynamic radii with increasing charge densities of anions in water–alcohol mixtures: (b) Miller, R. C.; Fuoss, R. M. *J. Am. Chem. Soc.* **1953**, *75*, 3076–80. (c) Reference 16a. (d) Franks, F.; Ives, D. J. G. *Quart. Rev.* **1966**, 1–44.

(18) Precise correlation between reduction potentials and kinetic and other physical data (e.g., outer-sphere reorganization energies) must include a description of phenomena, such as the solvent–solute interactions described here, that lie outside the assumptions of the dielectric continuum model used by Debye–Hückel and later by Marcus and others: (a) Werhland, S. *Coord. Chem. Rev.* **1993**, *123*, 169–199. (b) Chen, P.; Meyer, T. J. *Chem. Rev.* **1998**, *98*, 1439–1477.